THE JOURNAL OF BIOLOGICAL CHEMISTRY VOL. 281, NO. 4, pp. 2333–2337, January 27, 2006

Human SOD1 before Harboring the Catalytic Metal

SOLUTION STRUCTURE OF COPPER-DEPLETED, DISULFIDE-REDUCED FORM[*] [S]

Received for publication, June 15, 2005, and in revised form, October 3, 2005 Published, JBC Papers in Press, November 14, 2005, DOI 10.1074/jbc.M506497200

Lucia Banci[‡§], **Ivano Bertini**[‡§1], **Francesca Cantini**[‡], **Nicola D'Amelio**[‡¶], **and Elena Gaggelli**[¶]

From the [‡]*Magnetic Resonance Center, University of Florence, Via Luigi Sacconi 6, 50019 Sesto Fiorentino, Italy,* [§]*Department of Chemistry, University of Florence, Via della Lastruccia 3, 50019 Sesto Fiorentino, Italy, and* [¶]*Department of Chemistry, University of Siena, Via Aldo Moro, 53100 Siena, Italy*

SOD1 has to undergo several post-translational modifications before reaching its mature form. The protein requires insertion of zinc and copper atoms, followed by the formation of a conserved S–S bond between Cys-57 and Cys-146 (human numbering), which makes the protein fully active. In this report an NMR structural investigation of the reduced SH-SH form of thermostable E,Zn-*as*-SOD1 (E is empty; *as* is C6A, C111S) is reported, characterizing the protein just before the last step leading to the mature form. The structure is compared with that of the oxidized S–S form as well as with that of the yeast SOD1 complexed with its copper chaperone, CCS. Local conformational rearrangements upon disulfide bridge reduction are localized in the region near Cys-57 that is completely exposed to the solvent in the present structure, at variance with the oxidized forms. There is a local disorder around Cys-57 that may serve for protein-protein recognition and may possibly be involved in intermolecular S–S bonds in familial amyotrophic lateral sclerosis-related SOD1 mutants. The structure allows us to further discuss the copper loading mechanism in SOD1.

Cu,Zn-SOD[2] is a very efficient enzyme that catalyzes the dismutation of superoxide to oxygen and hydrogen peroxide (1). It is a dimer in all eukaryotes, whereas in prokaryotes it exists as either a dimer or a monomer. The mature, active form of SOD1 contains, in each subunit, a copper ion essential for catalysis and a zinc ion that has primarily a structural role.

In the active site, a narrow channel is present that is large enough to admit only superoxide, water, and small anions and ligands such as imidazole and peroxynitrite. In the lining of the channel there is a positively charged side chain from an arginine residue (Arg-143, human numbering). The cationic residue generates an electrostatic gradient proposed to be responsible for steering the superoxide anion toward the active site. Site-directed mutagenesis of residue 143 to a neutral or anionic residue produced proteins with dramatically reduced or abolished activity (2).

A peculiar feature of the mature form of SOD1 is the presence of a kinetically stable disulfide bond. Once formed, the disulfide bond is maintained in the reducing cytoplasmic environment where the majority of the SOD1 inside the cell is located. The presence of intramolecular disulfide bonds is common in secreted proteins, where their primary purpose is for protein stabilization. However, disulfide bonds are rare in intracellular proteins because of the highly reducing environment and low concentration of dioxygen in the cytosol (3, 4). It has been previously shown that intramolecular disulfide bonds in intracellular proteins (like SOD1) can play more than just a structural role and have functional significance (3). The disulfide bond between Cys-57 and Cys-146 is fully conserved in all SOD1 structures. This bond links loop IV, which contains Cys-57, with strand β8, containing Cys-146. The linkage of the secondary structure elements contributes to the stabilization of the SOD1 fold.

The active form of the protein is obtained when one zinc and one copper ion per subunit are bound. Although nothing is known on how the protein acquires the zinc ion, a description of the insertion of copper is available. The process is aided by a copper metallochaperone called CCS (copper chaperone for superoxide dismutase) (5, 6). Yeast mutants lacking CCS express a form of SOD1 protein that is essentially apo for copper but contains zinc (5, 7). However, a CCS-independent activation of mammalian SOD1 is possible (8). A mechanism of the copper transfer from CCS to SOD1 in yeast has been proposed based on the x-ray structure of the heterodimeric CCS-SOD1 complex (9). In this picture, SOD1 first loads zinc ions from an unknown source, and subsequently copper transfer takes place through the formation of an intermolecular S–S bond, involving Cys-57 of SOD1 and a Cys of CCS. The disulfide-reduced, copper-depleted form of SOD1 therefore represents the state of the protein before its complex formation with copper(I) CCS (10).

Additionally, this protein state may play a relevant role in pathological conditions. The presence of exposed cysteine residues may modulate its ability to interact with other macromolecules and to give rise to large molecular aggregates (11). Aggregates containing SOD1 have been found in some fALS patients and in some fALS SOD1 transgenic mice and rats (12, 13). The fALS pathology has been related to mutations in the protein Cu,Zn-SOD1, some of which have a tendency to form fibrils (14). An increasing number of pathological states involve protein aggregates, which represent the final state of biomolecules with altered folding properties and/or structural conformations (15). To avoid interference effects arising from Cys-6 and Cys-111 (*i.e.* the two other Cys present in SOD1 that are in the reduced state), we studied the thermostable mutant of human SOD1 (C6A, C111S), which is structurally and functionally equivalent to the wild type protein (16–18) and is commonly used in the study of fALS mutants to prevent intermolecular aggregation (4, 19–21).

* This work was supported by MIUR-COFIN 2003, UPMAN LSHG-CT-2004-512052, and the European Commission (QLG2-CT-2002-00988 and SPINE QLG2-CT-2002–00988). The costs of publication of this article were defrayed in part by the payment of page charges. This article must therefore be hereby marked "*advertisement*" in accordance with 18 U.S.C. Section 1734 solely to indicate this fact.

[S] The on-line version of this article (available at http://www.jbc.org) contains supplemental Figs. S1–S5 and supplemental Tables S1 and S2.

The atomic coordinates and structure factors (code 2AF2) have been deposited in the Protein Data Bank, Research Collaboratory for Structural Bioinformatics, Rutgers University, New Brunswick, NJ (http://www.rcsb.org/).

[1] To whom correspondence should be addressed. Tel.: 39-055-4574272; Fax: 39-055-4574271; E-mail: ivanobertini@cerm.unifi.it.

[2] The abbreviations used are: SOD, superoxide dismutase; CCS, copper chaperone for superoxide dismutase; fALS, familial amyotrophic lateral sclerosis; R_1, longitudinal relaxation rate; R_2, transversal relaxation rate; NOE, nuclear Overhauser effect; REM, restrained energy minimization; E,Zn-hSOD1^{SH-SH}, copper-depleted superoxide dismutase with reduced disulfide bridge; Cu,Zn-hSOD1^{SS}, superoxide dismutase with oxidized disulfide bridge; E,Zn-E133QM2-*as*SOD1^{SS}, monomeric form of copper-depleted superoxide dismutase with oxidized disulfide bridge.

Currently, there are a huge number of structures of SOD1 (>50, ~10 of which of human SOD1) deposited in the Protein Data Bank in various states (22–25), including several mutants, but all with the disulfide bond intact. Therefore, the structural characterization of E,Zn-SOD1 with the disulfide bond reduced that is reported here (hereafter E,Zn-h*as*SOD1$^{SH\text{-}SH}$) is particularly meaningful as it is the first structure of SOD1 with the disulfide bond broken. It represents the step before the protein acquires copper but also a state that is emerging to be relevant in the fALS-related SOD1 mutants (11, 26). Therefore, it provides useful new data on the features of SOD1.

MATERIALS AND METHODS

Sample Preparation—Human *as*SOD1 (h*as*SOD1) was expressed in the *Escherichia coli* TOPP1 (Stratagene) or BL21(DE3) strain. The ^{15}N and ^{15}N, ^{13}C, ^{2}H-labeled protein samples were obtained as previously reported (25). The protein was isolated and purified according to previously published protocols (16). The triple-labeled dimeric h*as*SOD1 contained ~70% ^{2}H. Metal ions were removed according to published protocols (27), and zinc reconstitution was obtained as described in Ref. 17. The reduction of disulfide bridge was accomplished by addition of dithiothreitol. Fully reduced and empty copper protein h*as*SOD1 (E,Zn-h*as*SOD1$^{SH\text{-}SH}$) was prepared under a nitrogen atmosphere in an anaerobic chamber. The thiol-disulfide status of purified h*as*SOD1 was determined by chemical modification with the thiol-specific reagent 4-acetamide-4′-maleimidylstilbene-2,2′-disulfonic acid (Molecular Probes, Inc.) (10).

The NMR samples of the E,Zn-h*as*SOD1$^{SH\text{-}SH}$ were in 20 mM sodium phosphate buffer, pH 5, 90% H_2O/10% D_2O. The final protein concentration ranges between 1 and 1.5 mM in the presence of 20 mM dithiothreitol. ~0.6 ml of sample was loaded into high quality NMR tubes that were capped with latex serum caps in the Vacuum Atmospheres chamber.

NMR Measurements and Structure Calculation—The NMR spectra were acquired on Avance 900, 800, 600, and 500 Bruker spectrometers. All of the triple resonance probes used were equipped with pulsed field gradients along the *z*-axis. The 800- and 500-MHz spectrometers were equipped with a triple resonance cryoprobe.

The NMR experiments, used for the backbone and the aliphatic side chain resonances assignment and for obtaining structural restraints, recorded on $^{2}H/^{13}C/^{15}N/$, $^{13}C/^{15}N$-enriched and unlabeled E,Zn-h*as*SOD1$^{SH\text{-}SH}$ samples, are summarized in supplemental Table S1. The ^{1}H, ^{13}C, and ^{15}N resonance assignments of E,Zn-h*as*SOD1$^{SH\text{-}SH}$ are reported in supplemental Table S2. In total, 88% of the ^{1}H, 98% of the ^{15}N, and 80% of the ^{13}C have been assigned. The combined variation of the ^{15}N and ^{1}H amide chemical shifts of E,Zn-h*as*SOD1$^{SH\text{-}SH}$, Cu,Zn-h*as*SOD1^{SS}, and E,Zn-E133QM2-*as*SOD1^{SS} are shown in supplemental Fig. S1.

^{1}H-^{1}H nuclear Overhauser enhancement spectroscopy (NOESY) experiment (80-ms mixing time) (28) was carried out to identify connectivities involving histidines of the binding sites at 298 K. All the spectra were collected at 298 K, processed using the standard Bruker software (XWINNMR), and analyzed through the CARA program (29).

An automated CANDID approach combined with DYANA torsion angle dynamics algorithm (30) was used to assign the ambiguous NOE cross-peaks and to have a preliminary protein structure. Structure calculations were then performed through iterative cycles of DYANA (31) followed by restrained energy minimization with AMBER 5.0 (32) applied to each member of the final DYANA family. The assessment of the structures was evaluated using the program PROCHECK-NMR (33). The root mean square deviation values for the backbone and heavy atoms of one subunit are shown in supplemental Fig. S2.

^{15}N R_1, R_2, and steady-state heteronuclear NOEs, which can provide information on internal mobility as well as on the overall protein tumbling rate, were measured with pulse sequences as described by Farrow *et al.* (34). R_2 were measured using a refocusing time of 450 ms. In all experiments the water signal was suppressed with the "water flip back" scheme (35). Average R_1, R_2, and ^{1}H-^{15}N NOE values of 0.81 ± 0.10, 23.7 ± 2.9, and 0.82 ± 0.10 s^{-1} are found, respectively, at 600 MHz. A correlation time of 17.3 ± 2.3 ns was estimated from the R_2/R_1 ratio (the experimental relaxation rates are shown in supplemental Fig. S3).

The exchange with the solvent of the backbone amide proton was investigated through a series of ^{1}H-^{15}N heteronuclear single quantum correlation (HSQC) experiments performed over 4 days on the E,Zn-h*as*SOD1$^{SH\text{-}SH}$ protein previously frozen dry and then dissolved in D_2O. Exchange with the bulk solvent in D_2O solution was measured following the intensity of amide proton moieties in ^{15}N-HSQC spectra. The amide protons can be grouped in three groups: fast exchanging (the peak disappears in less than 20 min), intermediate exchanging (the peak is still present after 20 min but disappears within 10 h), and slow exchanging (the peak persists after 10 h). The behavior indicates not only solvent exposure but also the presence of hydrogen bonding, which may slow down the exchange of the exposed amide protons. This is the case for almost all residues located in regions having a defined secondary structure, as they are involved in extensive H-bond networks that stabilize the β-barrel structure typical of this protein.

Copper(I) Insertion—The copper-depleted protein was added with the copper(I) complex $(Cu(CH_3CN)_4)^+$ in a 1:1 ratio in an anaerobic chamber. The protein was then washed extensively in the presence of phosphate buffer 20 mM at pH 5. The metal uptake of the protein was established through one-dimensional NMR spectrum in the region of imidazole NHs (10–16 ppm).

RESULTS AND DISCUSSION

The structure of the copper-depleted thermostable form (C6A, C111S) of human SOD1 with the disulfide bond reduced (E,Zn-h*as*SOD1$^{SH\text{-}SH}$) has been determined in solution by NMR with high resolution (root mean square deviation 0.66 ± 0.14 and 1.15 ± 0.13 for the backbone and heavy atom, respectively, considering the segments involved in the β-barrel). The structure quality and the statistics on constraint violations for the final family is shown in Table 1. The protein is in a dimeric state and completely maintains the global fold of mature SOD1 (Fig. 1). Surprisingly, the breakage of the disulfide bond does not significantly destabilize the protein structure. This can suggest a functional rather than structural role for this highly conserved moiety. In addition, the backbone conformation of the region at the dimer interface (residues 53–55, 149–151) is very similar to that found in x-ray (22, 36) and solution structures (25) of human and yeast Cu,Zn-SOD1^{SS}. Local conformational rearrangements are found essentially only in the immediate surrounding of the two cysteines (Cys-57 and -146) involved in the intrasubunit disulfide bond. This protein region, and in particular residue 57, becomes extremely more solvent accessible with respect to the oxidized protein (Fig. 2). The solvent exposure of cysteine 57 is a peculiarity that is never observed in SOD1 structures, not even in the apo form of the protein (Fig. 2 and supplemental Fig. S4). The presence of the disulfide bond, in fact, prevents solvent exposure by forcing the Cys-57 to reach the Cys-146 that is located within the protein core. Solvent exposure is also confirmed by H_2O/D_2O solvent exchange measurements. The region spatially close to the cysteine residues responsible for the disulfide bridge (residues 57 and 146) appears more

TABLE 1
Statistical analysis of the energy-minimized family of conformers and the mean structure of E, Zn-h*as*SOD1^{SH-SH}

	REM[a]	⟨REM⟩[a]
Root mean square violations per meaningful distance constraint (Å)[b]	(30 structures)	(mean)
Intraresidue (554)	0.0184 ± 0.0016	0.0215
Sequential (1496)	0.0099 ± 0.0014	0.0102
Medium range (1023)[c]	0.0107 ±0.0014	0.0096
Long range (2734)	0.0102 ± 0.0013	0.0079
Total (5807)	0.0113 ± 0.0009	0.0108
Root mean square violations per meaningful dihedral angle constraints (deg)[b]		
Phi (183)	2.72 ± 1.76	1.98
Psi (162)	2.67 ± 1.02	2.11
Average number of constraints per residue	19	
Average number of violations per structure		
Intraresidue	25.2 ± 2.5	26
Sequential	25.4 ± 3.9	30
Medium range	19.2 ± 3.3	18
Long range	45.7 ± 3.9	30
Total	115.5 ± 7.2	104
Phi	18.6 ± 2.7	14
Psi	14.4 ± 2.9	12
Average no. of NOE violations larger than 0.3 Å	0.02 ± 0.17	0
Average no. of NOE violations between 0.1 Å and 0.3 Å	16.88 ± 4.241	15
Average NOE target function (Å^2)	0.88 ± 0.14	0.82
Average angle target function (rad^2)	0.80 ± 0.50	0.48
Structural analysis[d]		
% of residues in most favorable regions	65.0%	67.6%
% of residues in allowed regions	29.1%	27.3%
% of residues in generously allowed regions	5.2%	4.2%
% of residues in disallowed regions	0.8%	0.8%
Secondary structure elements (residues 1–153)	β1 (3–6), β2 (15–21), β3 (29–37), B4 (41–48), β5 (85–89), β6 (94–101), β7 (116–121), α1 (131–137), β8 (143–152)	

[a] REM indicates the energy minimized family of 30 structures, ⟨REM⟩ is the energy-minimized mean structure obtained from the coordinates of the individual REM structures.
[b] The number of meaningful constraints for each class is reported in parentheses.
[c] Medium range distance constraints are those between residues (i,i+2), (i,i+3), (i,i+4), and (i,i+5).
[d] As it results from the Ramachandran plot analysis.

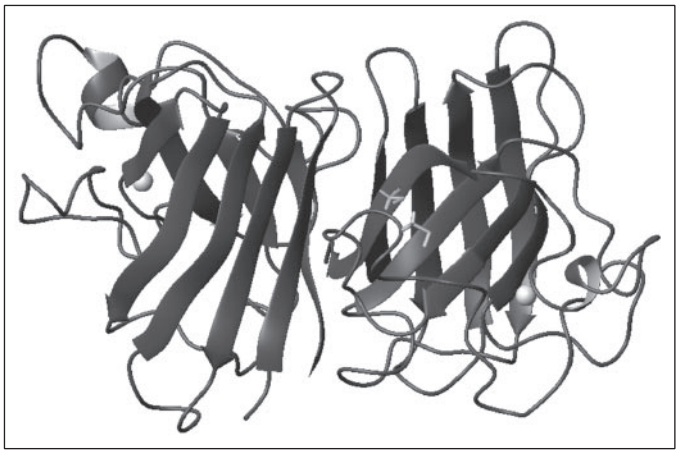

FIGURE 1. **Solution structure of E,Zn-h*as*SOD1^{SH-SH}.** The side chains of Cys-57 and Cys-146 are shown as *sticks*.

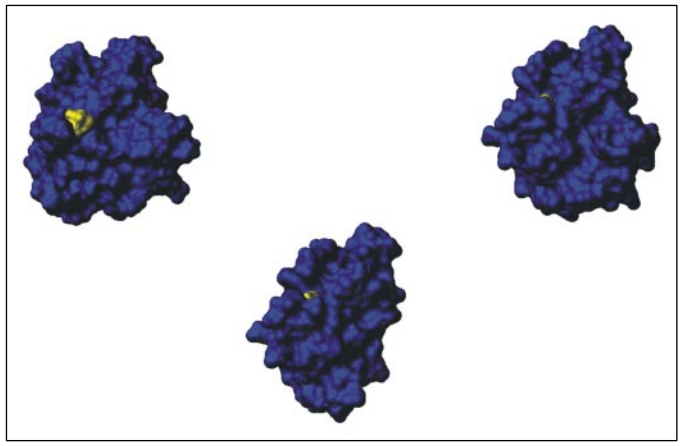

FIGURE 2. **Solvent exposure of Cys-57 in the structures of one subunit of thermostable E,Zn-h*as*SOD1^{SH-SH} (*left*), Cu,Zn-h*as*SOD1^{SS} (*right*; Protein Data Bank code 1SOS), and wild type E,E-hSOD1^{SS} (*center*; Protein Data Bank code 1HL4).** The surface of Cys-57 is shown in *lighter color*.

exposed to the solvent. This was not observed in the structures of Cu,Zn-h*as*SOD1^{SS} and E,Zn-E133QM2-*as*SOD1^{SS}.

Interestingly, the metal binding ligands in E,Zn-h*as*SOD1^{SH-SH} have a conformation very close to that found in Cu,Zn-h*as*SOD1^{SS} and in the monomeric copper-depleted form (24, 25), indicating that the protein is ready to harbor the catalytic metal. In the active site channel of Cu,Zn-SOD1^{SS}, located between the electrostatic loop VII (121–142) and loop IV (49–84), some H-bonds form a highly conserved network that is important for generating the optimal electrostatic field necessary to attract and drive the substrate toward the copper site. In the present structure most of the H-bonds are maintained with the exceptions of the copper ligand His-48 hydrogen bonded to Cys-57 via the carbonyl oxygen of Gly-61 and the catalytically important side chain of Arg-143. This is also assessed by the chemical shift perturbation of the amide proton of Gly-61 (supplemental Fig. S1). The total solvent exposure of Cys-57 located in loop IV is also reflected in an increased solvent exposure of residues 48 and 146, which are buried in Cu,Zn-hSOD1^{SS}. Accordingly, the relative amide protons display fast hydrogen/deuterium exchange in E,Zn-h*as*SOD1^{SH-SH} (data not shown).

The conformation of Arg-143 is extremely sensitive to the position of Cys-57 (37–39). Arg-143 is located at the end of the electrostatic loop (loop VII) whose conformation greatly affects the enzymatic activity. In the dimeric Cu,Zn-h*as*SOD1^{SS} solution structure, Cys-57 is quite rigid along with loop VII. As a consequence, the side chain of Arg-143 is highly ordered and is in the optimal conformation to interact with the

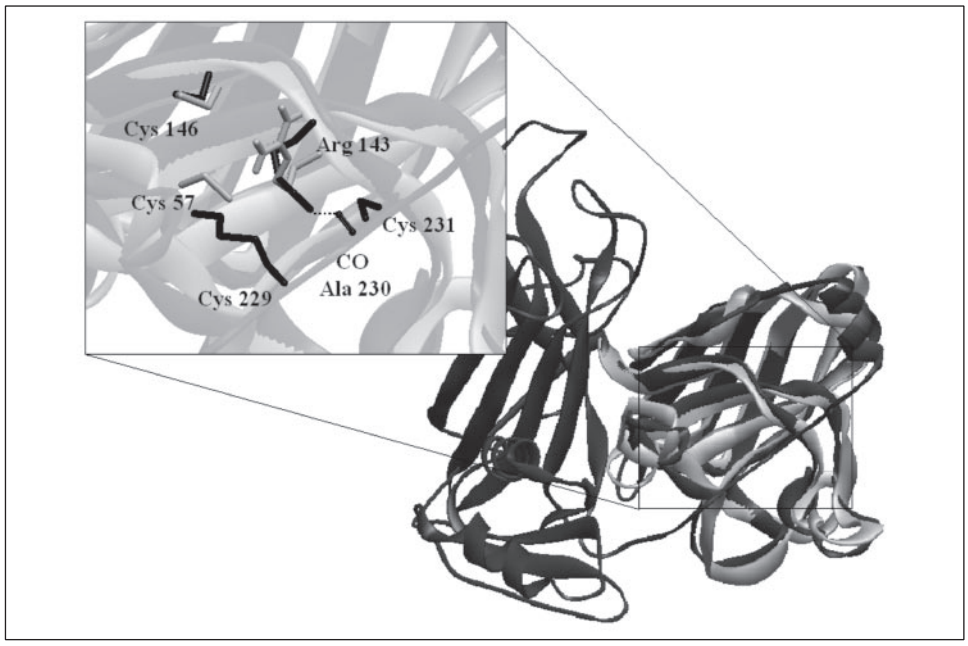

FIGURE 3. **Structure superimposition of E,Zn-h*as*SOD1$^{SH\text{-}SH}$ (*light gray*) and yeast SOD1 interacting with yeast CCS (*black*).** Some key residues are highlighted (*gray* for E,Zn-h*as*SOD1$^{SH\text{-}SH}$ and *black* for yeast SOD1): the carbonyl of Ala-230 involved in an H-bond with Arg-143 in the yeast complex, Cys-229 and Cys-231 belonging to CCS, Cys-57 and Cys-146 belonging to SOD1 structures.

superoxide anion bound to copper. In the monomeric Cu,Zn-E133QM2-*as*SOD1^{SS} species, loop IV containing Cys-57 experiences conformational equilibria and Arg-143 moves away from copper, determining a sizable drop in SOD activity (40). In the present structure, loop IV is highly disordered due to the S–S breaking resulting in extensive disorder of the Arg-143 side chain. Consequently, the overall electrostatic field is highly perturbed. The comparison of our solution structure with that of monomeric E,ZnE133QM2-*as*SOD1^{SS} (24) reveals that the observed disorder of residue Arg-143 is not a consequence of the absence of copper but of the relaxation of loop IV due to the S–S breaking. The breakage of the disulfide bond results in a perturbed distribution of the electrostatic charges in the active site channel essential to guide the superoxide ion in the catalytic site.

Two mechanisms have been proposed for copper uptake and consequent activation of human SOD1; the first requires the presence of CCS (9, 41), and the second involves the reduced form of glutathione (8). The first mechanism, described in yeast, is based on the x-ray structure of the heterodimeric yeast CCS-SOD1 complex. Although a direct comparison with the yeast E,Zn-SOD1$^{SH\text{-}SH}$ is not possible because of the lack of its structure in the Protein Data Bank, the present solution structure shares some specific features with that of the yeast mutant H48F SOD1 in the heterodimeric complex with CCS (9) (Fig. 3). All SOD1 residues involved in the interaction with domain II of CCS (residues 51, 114, 152) experience similar conformation in E,Zn-h*as*SOD1$^{SH\text{-}SH}$ regardless of the differences in the primary sequence. It has been proposed that in yeast the presence of Pro-142 and Pro-144 in place of Ser-142 and Leu-144 may account for the loss of ability to acquire copper independently of CCS (8). Because yeast E,Zn-SOD1$^{SH\text{-}SH}$ has been found to be monomeric (10), we can speculate that these differences in the primary sequence destabilize the structure of this region, leading to monomerization (Leu-144 is inserted in the hydrophobic part of the protein called the plug of the barrel). The correct conformation for acquiring copper could be restored only by the formation of the heterodimeric complex with CCS facilitated by interaction with domain III. However, the complexity of the issue is demonstrated by the increased propensity to monomerization displayed by a subgroup of fALS mutants (for example G85R, D125H, L38V) that have the mutation far away from the dimer interface (11, 19, 26).

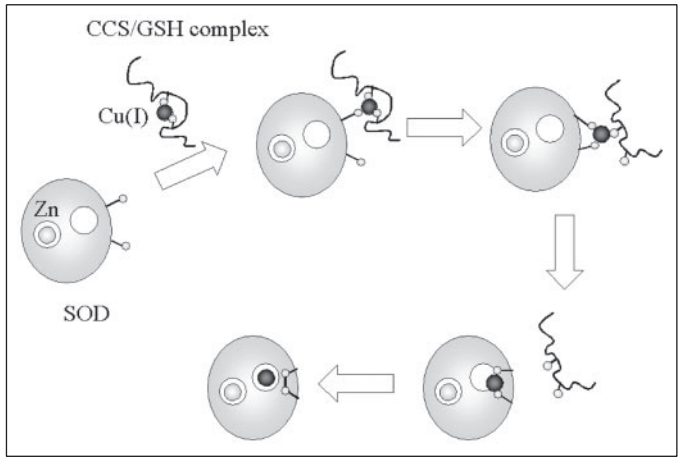

FIGURE 4. **Proposed mechanism for acquisition of copper by E,Zn-hSOD1$^{SH\text{-}SH}$ (displayed as an *ellipsoid*).** Copper and zinc are represented as *spheres* (*dark* and *light gray*, respectively) and their sites as *empty circles*. Thiol groups are shown as *small spheres*. A hypothetical mechanism for acquisition of copper ion from CCS or glutathione (*GSH*) complex (shown as a *thick wavy line*) could take place through the formation of a metal-bridged intermediate.

In the crystal structure of the heterodimeric complex, an intermolecular disulfide bond between Cys-57 of SOD1 and Cys-229 of CCS was found. If the present solution structure is superimposed on the yeast H48F SOD1 in the heterodimeric complex, a similar distance of the sulfur atom of Cys-57 from that of Cys-229 of CCS is found (0.20 nm in the heterodimer complex and 0.28 nm in the superimposed solution structure of E,Zn-h*as*SOD1$^{SH\text{-}SH}$). This feature demonstrates that Cys-57 has a favorable conformation to form the same disulfide bond. Also, in the heterodimer complex the side chain of Arg-143 is far away from the copper site and is hydrogen bonded to the backbone of Ala-230 of yeast CCS; the mobility of Arg-143 could have the role of making its side chain available for this kind of interaction.

On the basis of the present structure we can speculate that the copper ion could enter in its site with the assistance of Cys-57, which, being close to the copper site, could constitute a ligand in a hypothetical intermediate (Fig. 4). Indeed, the high affinity of copper for thiol groups and the complete exposure of the side chain of Cys-57 could be significant

for the incorporation of copper ion into the protein, regardless of whether this occurs through the interaction with CCS (9, 41) or with other copper-containing species (*e.g.* copper-glutathione complex) (8).

Independently of the mechanism by which the copper enters the site *in vivo*, we have observed that E,Zn-h*as*SOD1$^{SH\text{-}SH}$ is able to acquire copper(I) *in vitro*. The acquisition of copper can, in fact, be easily monitored by one-dimensional NMR spectrum of imidazole NH protons. Supplemental Fig. S5 shows the signals originated by copper binding; the figure also shows that the spectra of Cu(I),Zn-h*as*SOD1$^{SH\text{-}SH}$ and Cu(I),Zn-hSOD1^{SS} are very similar (and different from E,Zn-h*as*SOD1$^{SH\text{-}SH}$), thus demonstrating that the metal enters correctly in its site. Subsequent oxidation of the disulfide bond would allow the formation of the hydrogen bond network constraining the side chain of Arg-143, making the protein fully functioning.

Exposed cysteines can also easily form interprotein disulfide bonds, thus giving rise to aggregates. The status of the disulfide bond in fALS SOD1 mutants has not been extensively characterized, although in all crystal structures of fALS mutants such bonds are intact (42–44). However, the disulfide bonds in fALS mutants are more susceptible to reduction than wild type SOD1 (26), and it has been suggested that in some fALS mutants, fibrils are formed through intersubunit S–S bonds (11). This implies that under cellular disulfide-reducing conditions at physiological pH and temperature, the fALS SOD1 mutants are more prone to aggregation. The present structure provides an important piece of information for understanding the copper uptake mechanism in SOD1 and for the debate about which is the relevant form of SOD1 for the onset of the fALS pathology.

REFERENCES

1. Fridovich, I. (1986) *Adv. Enzymol. Relat. Areas Mol. Biol.* **58,** 61–97
2. Banci, L., Bertini, I., Luchinat, C., and Hallewell, R. A. (1988) *J. Am. Chem. Soc.* **110,** 3629–3633
3. Sevier, C. S., and Kaiser, C. A. (2002) *Nat. Rev. Mol. Cell. Biol.* **3,** 836–847
4. Valentine, J. S., Doucette, P. A., and Potter, S. Z. (2004) *Annu. Rev. Biochem.*
5. Culotta, V. C., Klomp, L. W., Strain, J., Casareno, R. L., Krems, B., and Gitlin, J. D. (1997) *J. Biol. Chem.* **272,** 23469–23472
6. Portnoy, M. E., Schmidt, P. J., Rogers, R. S., and Culotta, V. C. (2001) *Mol. Genet. Genomics* **265,** 873–882
7. Wong, P. C., Waggoner, D., Subramaniam, J. R., Tessarollo, L., Bartnikas, T. B., Culotta, V. C., Price, D. L., Rothstein, J., and Gitlin, J. D. (2000) *Proc. Natl. Acad. Sci. U. S. A.* **97,** 2886–2891
8. Carroll, M. C., Girouard, J. B., Ulloa, J. L., Subramaniam, J. R., Wong, P. C., Valentine, J. S., and Culotta, V. C. (2004) *Proc. Natl. Acad. Sci. U. S. A.* **101,** 5964–5969
9. Lamb, A. L., Torres, A. S., O'Halloran, T. V., and Rosenzweig, A. C. (2001) *Nat. Struct. Biol.* **8,** 751–755
10. Furukawa, Y., Torres, A. S., and O'Halloran, T. V. (2004) *EMBO J.* **23,** 2872–2881
11. Furukawa, Y., and O'Halloran, T. V. (2005) *J. Biol. Chem.* **280,** 17266–17274
12. Wang, J., Slunt, H., Gonzales, V., Fromholt, D., Coonfield, M., Copeland, N. G., Jenkins, N. A., and Borchelt, D. R. (2003) *Hum. Mol. Genet.* **12,** 2753–2764
13. Johnston, J. A., Dalton, M. J., Gurney, M. E., and Kopito, R. R. (2000) *Proc. Natl. Acad. Sci. U. S. A.* **97,** 12571–12576
14. Rowland, L. P., and Shneider, N. A. (2001) *N. Eng. J. Med.* **344,** 1688–1700
15. Taylor, J. P., Hardy, J., and Fischbeck, K. H. (2005) *Science* **296,** 1991–1995
16. Hallewell, R. A., Imlay, K. C., Laria, I., Gallegos, C., Fong, N. M., Irvine, B., Cabelli, D. E., Bielski, B. H. J., Olson, P., Mullenbach, G. T., and Cousens, L. S. (1991) *Biochem. Biophys. Res. Commun.* **181,** 474–480
17. Lepock, J. R., Frey, H. E., and Hallewell, R. A. (1990) *J. Biol. Chem.* **265,** 21612–21618
18. Parge, H. E., Hallewell, R. A., and Tainer, J. A. (1992) *Proc. Natl. Acad. Sci. U. S. A.* **89,** 6109–6114
19. Lindberg, M. J., Bystrom, R., Boknas, N., Andersen, P. M., and Oliveberg, M. (2005) *Proc. Natl. Acad. Sci. U. S. A.* **102,** 9754–9759
20. Stathopulos, P. B., Rumfeldt, J. A., Scholz, G. A., Irani, R. A., Frey, H. E., Hallewell, R. A., Lepock, J. R., and Meiering, E. M. (2003) *Proc. Natl. Acad. Sci. U. S. A.* **100,** 7021–7026
21. Banci, L., Bertini, I., D'Amelio, N., Gaggelli, E., Libralesso, E., Matecko, I., Turano, P., and Valentine, J. S. (2005) *J. Biol. Chem.* **280,** 35815–35821
22. Strange, R. W., Antonyuk, S., Hough, M. A., Doucette, P. A., Rodriguez, J. A., Hart, P. J., Hayward, L. J., Valentine, J. S., and Hasnain, S. S. (2003) *J. Mol. Biol.* **28,** 877–882
23. Banci, L., Bertini, I., Cramaro, F., Del Conte, R., and Viezzoli, M. S. (2003) *Biochemistry* **42,** 9543–9553
24. Banci, L., Bertini, I., Cantini, F., D'Onofrio, M., and Viezzoli, M. S. (2002) *Protein Sci.* **11,** 2479–2492
25. Banci, L., Bertini, I., Cramaro, F., Del Conte, R., and Viezzoli, M. S. (2002) *Eur. J. Biochem.* **269,** 1905–1915
26. Tiwari, A., and Hayward, L. J. (2003) *J. Biol. Chem.* **278,** 5984–5992
27. McCord, J. M., and Fridovich, I. (1969) *J. Biol. Chem.* **244,** 6049–6055
28. Wider, G., Macura, S., Kumar, A., Ernst, R. R., and Wüthrich, K. (1984) *J. Magn. Reson.* **56,** 207–234
29. Keller, R. L. J. *The Computer-aided Resonance Assignment Tutorial* (1.3) (2004) Cantina Verlag
30. Herrmann, T., Güntert, P., and Wüthrich, K. (2002) *J. Mol. Biol.* **319,** 209–227
31. Guntert, P., Mumenthaler, C., and Wüthrich, K. (1997) *J. Mol. Biol.* **273,** 283–298
32. Pearlman, D. A., Case, D. A., Caldwell, J. W., Ross, W. S., Cheatham, T. E., Ferguson, D. M., Seibel, G. L., Singh, U. C., Weiner, P. K., and Kollman, P. A. (1997) *AMBER 5.0*, University of California, San Francisco
33. Laskowski, R. A., Rullmann, J. A. C., MacArthur, M. W., Kaptein, R., and Thornton, J. M. (1996) *J. Biomol. NMR* **8,** 477–486
34. Farrow, N. A., Muhandiram, R., Singer, A. U., Pascal, S. M., Kay, C. M., Gish, G., Shoelson, S. E., Pawson, T., Forman-Kay, J. D., and Kay, L. E. (1994) *Biochemistry* **33,** 5984–6003
35. Grzesiek, S., and Bax, A. (1993) *J. Am. Chem. Soc.* **115,** 12593–12594
36. Hart, J. P., Balbirnie, M. M., Ogihara, N. L., Nersissian, A. M., Weiss, M. S., Valentine, J. S., and Eisenberg, D. (1999) *Biochemistry* **38,** 2167–2178
37. Banci, L., Carloni, P., La Penna, G., and Orioli, P. L. (1992) *J. Am. Chem. Soc.* **114,** 6994–7001
38. Banci, L., Bertini, I., Del Conte, R., and Viezzoli, M. S. (1999) *Biospectroscopy* **5,** 33–41
39. Banci, L., Bertini, I., Del Conte, R., Mangani, S., Viezzoli, M. S., and Fadin, R. (1999) *J. Biol. Inorg. Chem.* **4,** 795–803
40. Banci, L., Benedetto, M., Bertini, I., Del Conte, R., Piccioli, M., and Viezzoli, M. S. (1998) *Biochemistry* **37,** 11780–11791
41. Lamb, A. L., Torres, A. S., O'Halloran, T. V., and Rosenzweig, A. C. (2000) *Biochemistry* **39,** 14720–14727
42. Antonyuk, S., Elam, J. S., Hough, M. A., Strange, R. W., Doucette, P. A., Rodriguez, J. A., Hayward, L. J., Valentine, J. S., Hart, P. J., and Hasnain, S. S. (2005) *Protein Sci.* **14,** 1201–1213
43. Hart, P. J., Liu, H., Pellegrini, M., Nersissian, A. M., Gralla, E. B., Valentine, J. S., and Eisenberg, D. (1998) *Protein Sci.* **7,** 545–555
44. Elam, J. S., Taylor, A. B., Strange, R., Antonyuk, S., Doucette, P. A., Rodriguez, J. A., Hasnain, S. S., Hayward, L. J., Valentine, J. S., Yeates, T. O., and Hart, P. J. (2003) *Nature Struct. Biol.* **10,** 461–467

Human SOD1 before Harboring the Catalytic Metal: SOLUTION STRUCTURE OF COPPER-DEPLETED, DISULFIDE-REDUCED FORM

Lucia Banci, Ivano Bertini, Francesca Cantini, Nicola D'Amelio and Elena Gaggelli

J. Biol. Chem. 2006, 281:2333-2337.
doi: 10.1074/jbc.M506497200 originally published online November 14, 2005